ARTICLE IN PRESS

Ceramics International xxx (xxxx) xxx-xxx

ELSEVIER

Contents lists available at ScienceDirect

Ceramics International

journal homepage: www.elsevier.com/locate/ceramint



Effects of post-sintering annealing on the microstructure and toughness of hot-pressed SiC_f/SiC composites with $Al_2O_3-Y_2O_3$ additions

Pipit Fitriani, Dang-Hyok Yoon, Amit Siddharth Sharma*

School of Materials Science and Engineering, Yeungnam University, 38541, South Korea

ARTICLE INFO

Keywords: Ceramic matrix composites SiC Flexural strength Toughness and toughening

ABSTRACT

This study examined the effects of post-sintering heat treatment on enhancing the toughness of SiC $_f$ /SiC composites. Commercially available Tyranno $^\circ$ SiC fabrics with contiguous dual 'PyC (inner)-SiC (outer)' coatings deposited on the SiC fibers were infiltrated with a SiC + 10 wt% Al $_2$ O $_3$ -Y $_2$ O $_3$ slurry by electrophoretic deposition. SiC green tapes were stacked between the slurry-infiltrated fabrics to control the matrix volume fraction. Densification of approximately 94% ρ_{theo} was achieved by hot pressing at 1750 °C, 20 MPa for 2 h in an Ar atmosphere. Sintered composites were then subjected to isothermal annealing treatment at 1100, 1250, 1350, and 1750 °C for 5 h in Ar. The correlation between the flexural behavior and microstructure was explained in terms of the in situ-toughened matrix, phase evolution in the sintering additive, role of dual interphases and observed fracture mechanisms. Extensive fractography analysis revealed interfacial debonding at the hybrid interfaces and matrix cracking as the key fracture modes, which were responsible for the toughening behavior in the annealed SiC $_f$ /SiC composites.

1. Introduction

Silicon carbide (SiC)-based ceramics are one of the most attractive materials owing to their stable strength at high temperatures (> 1500 °C), low specific mass, chemical inertness, and corrosion resistance [1]. In addition, continuous SiC fiber-reinforced SiC matrix (SiC_f/ SiC) composites have been proposed as a prime candidate for the structural components in future fusion and advanced fission reactors because of their low induced radioactivity, good resistance under neutron irradiation, and limited saturation swelling [1-3]. On the other hand, the fabrication of high density, damage-tolerant SiC_f/SiC composites poses a formidable challenge to material scientists considering its covalent nature and inherent brittleness. Near theoretical densification of SiC green compacts can be attained by resorting to liquid phase sintering (LPS). Sintering additives based on metals [4], metal oxides [5,6], glass compositions [7], and rare earth elements [8– 11] have been quite promising in improving the sintering conditions to 1700-1800 °C/30-40 MPa compared to those without an additive (~2500 °C/5 GPa) [12]. Damage-tolerance attributes such as pseudoductile behavior and a predictable fracture mode in SiC_f/SiC composites can be achieved by tailoring a 'weak' PyC or hBN interface between the matrix and reinforcement fabric [13,14]. In SiC monoliths, the possibility of having heterogeneous microstructure with respect to phase and size distribution of SiC grains has been proposed to be effective for in situ-toughening. Incorporation of α -SiC seeds in β -SiC matrix and/or post-sintering treatments in the temperature range 1850–2000 °C to promote $\beta \rightarrow \alpha$ SiC transformation have been extensively investigated for SiC monoliths [15-23]. Exaggerated grain growth due to high temperature heat treatment (HT) can also lead to the increase in critical flaw size which adversely affects the flexural strength and hence annealing should preferably be performed at lower temperatures. Effects of annealing on additives-borne grain boundary (GB) phases also needs to be controlled as the morphology of these secondary phases influence the oxidation resistance, creep resistance, and high-temperature strength [24-32]. Post-sintering annealing studies on SiC monolithic ceramics with Al₂O₃ and Y₂O₃ relates mechanical properties to evolution of GB phases and asserted on the importance of Al₂O₃:Y₂O₃ ratio, processing variables (time, temperature, and atmosphere), and characteristics of the initial powders (phases, morphology, and size ranges). The incipient SiO2 layer on the SiC powders reacting with Al₂O₃ and Y₂O₃ powders can yield a number of phases dictated by ternary Al₂O₃-Y₂O₃-SiO₂ phase diagram [24,29-34].

In this study, SiC_f/SiC composites were prepared from Tyranno SiC fabric having dual PyC-SiC coating on the SiC fibers with controllable fraction of SiC matrix and 10 wt% Al_2O_3 - Y_2O_3 as the sintering additive. The main aim of this study was to extend the applicability of post-sintering heat treatments (HTs) to SiC_f/SiC

E-mail address: amitsidd@ynu.ac.kr (A.S. Sharma).

http://dx.doi.org/10.1016/j.ceramint.2017.07.031

Received 6 April 2017; Received in revised form 4 July 2017; Accepted 4 July 2017 0272-8842/ © 2017 Elsevier Ltd and Techna Group S.r.l. All rights reserved.

^{*} Corresponding author.

P. Fitriani et al. Ceramics International xxx (xxxx) xxx-xxx

composites. These low temperature heat treatments were designed judiciously such that the formation and volume fraction of detrimental phases and interfacial damage can be minimized in the three constituents, i.e., matrix, reinforcement and interphases. Heat treatments were optimized such that the composites display maximum toughening behavior in flexure. Further comparative analyses based on the respective fracture mechanisms, phase assemblage, and fracture energies were established.

2. Experimental methods

Commercially available $\beta\text{-SiC}$ nanopowder (> 97.5% purity, $D_{50}\sim52$ nm, 4620KE, NanoAmor Inc., USA) and Tyranno $^{\circ}$ SA3 fabrics (Ube Industries Ltd., Japan) were used as the starting materials. An inner 300 nm-thick PyC layer by the decomposition of methane (CH $_4$) at 1100 °C and an outer 400 nm-thick SiC layer by the decomposition of methyl tetrachlorosilane (MTS) at 1000 °C were deposited on SiC fibers by chemical vapor deposition. Details of slurry preparation and steps involved in composites fabrication can be referred from earlier published works [35]. Post-sintering thermal treatments were carried out at 1150, 1250, 1350, and 1750 °C for 5 h in a flowing Ar atmosphere without the application of pressure.

Characterization: The hot-pressed flat samples of dimensions $30 \times 30 \times 2 \ (\mathrm{mm^3})$ were cut into $30 \times 4 \times 2 \ (\mathrm{mm^3})$ bars with approximately 5 bars for each HT condition and fine polished for the 3-point bending test (UTM AG-50E, Shimadzu, Japan). To delineate the grain boundaries, polished samples were etched thermally at 1400 °C for 30 min. Microstructural analyses and fractured surfaces were examined by scanning electron microscopy (SEM; Hitachi S-4800). Nano-thin lamellae for transmission electron microscopy (TEM; Titan G2 ChemiSTEM, FEI Company) was prepared by focused ion beam (FIB; Versa3D LoVac, FEI Company) sectioning using Ga⁺ ions with milling and polishing runs conducted at $30 \ \mathrm{kV}$, $100 \ \mathrm{pA}$ and $5 \ \mathrm{kV}$, $77 \ \mathrm{pA}$,

respectively. After a final polish, the lamellae was lifted-off by a tungsten tip (OmniProbe 400; Oxford Instruments) and attached to a sample grid for TEM examination.

3. Results and discussion

3.1. Microstructural analyses and phase assemblage

Fig. 1(a) shows secondary electron (SE)-SEM images of the fiber bundle in SiC fabric with smooth and well-adherent PvC-SiC coatings with uniform thicknesses around the SiC fibers (see inset). Fig. 1(b) revealed efficient SiC matrix infiltration down to the level of the SiC fiber bundles at sintering temperature. Fig. 1(c) presents XRD pattern of the polished surfaces of the as-sintered and post-sintering heattreated samples; peaks of each phase were indexed using the ICDD° (International Centre for Diffraction Data) database. After sintering, distinct peaks of Y₃Al₅O₁₂ (YAG) and Y₃Al₃O₉ (YAP) phase resulting from Al₂O₃-Y₂O₃ addition as well as α - and β -SiC phases were detected. In Fig. 2(a), bright field transmission electron microscope (BF-TEM) image of the matrix region shows a well-packed pore-free microstructure containing equiaxed SiC grains with a mean size close to 500 nm. The Z-contrast high-angle annular dark field (HAADF) image and its corresponding elemental map in Fig. 2(b) confirmed Al- and Y-based sintering additive located at the intergranular pockets around the SiC grains. In addition to having an equiaxed morphology (marked '+'), the additive phases also occur as thin intergranular films (IGF) with a mean thickness of less than 7 nm (marked by arrows). The contrast inside the SiC grains can be attributed to the presence of stacking faults; the results of detailed investigation into the ordering sequence have not been included here. Table 1 lists the designated notation and results of a quantitative Rietveld evaluation of volume fraction of each phase in the composites corresponding to each heat treatment temperatures.

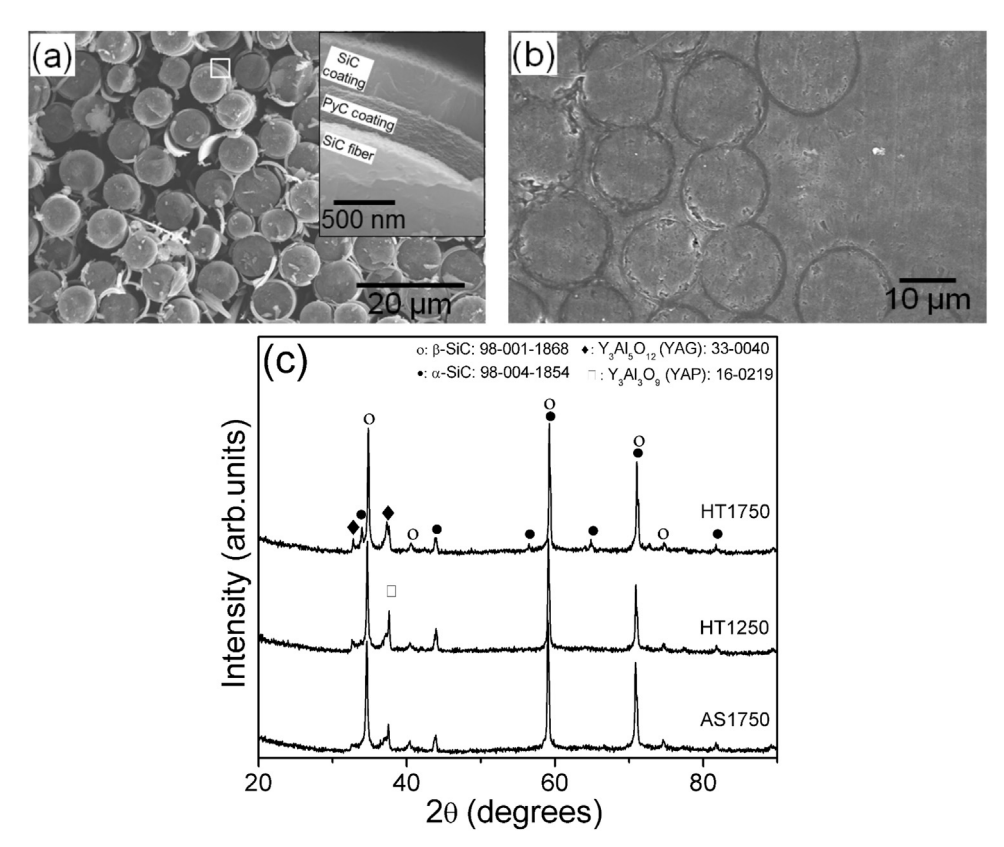


Fig. 1. SE-SEM image of the a) fiber bundle in the fabric (transverse view), b) sintered SiC_i/SiC composite and c) XRD patterns of the sintered and heat-treated composites. Inset in a) showing the dual PyC-SiC coating.

Download English Version:

https://daneshyari.com/en/article/5437830

Download Persian Version:

https://daneshyari.com/article/5437830

<u>Daneshyari.com</u>